

AD-A053 786

NAVAL RESEARCH LAB WASHINGTON D C
INTENSE PROTON BEAM PUMPED AR-N2 LASER.(U)
APR 78 J G EDEN, J GOLDEN, R A MAHAFFEY
NRL-MR-3761

F/G 20/5

UNCLASSIFIED

NL

| OF |

AD
A053 786



END
DATE
FILMED
6-78
DDC

AD A 053786

AD No. _____

DDC FILE COPY

NRL Memorandum Report 3761

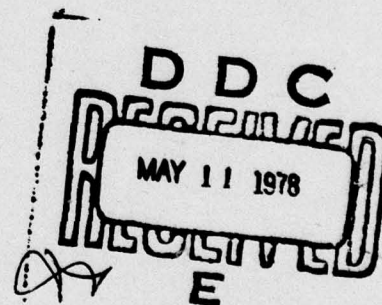
(12)

Intense Proton Beam Pumped Ar-N₂ Laser

J. G. EDEN, J. GOLDEN, R. A. MAHAFFEY, J. A. PASOUR,
A. W. ALI and C. A. KAPETANAKOS

*Experimental Plasma Physics Branch
Plasma Physics Division*

April 1978



NAVAL RESEARCH LABORATORY
Washington, D.C.

SECURITY CLASSIFICATION OF THIS PAGE (When Data Entered)

REPORT DOCUMENTATION PAGE		READ INSTRUCTIONS BEFORE COMPLETING FORM	
1. REPORT NUMBER NRL Memorandum Report 3761	2. GOVT ACCESSION NO.	3. RECIPIENT'S CATALOG NUMBER	
4. TITLE (and Subtitle) INTENSE PROTON BEAM PUMPED Ar-N₂ LASER		5. TYPE OF REPORT & PERIOD COVERED Interim report on a continuing NRL problem	
6. AUTHOR(s) J. G. Eden, J. Golden, R. A. Mahaffey, J. A. Pasour, A. W. Ali and A. A. Kapetanakis		6. PERFORMING ORG. REPORT NUMBER	
7. PERFORMING ORGANIZATION NAME AND ADDRESS Naval Research Laboratory Washington, D.C. 20375		8. CONTRACT OR GRANT NUMBER(s)	
9. CONTROLLING OFFICE NAME AND ADDRESS Office of Naval Research Arlington, Virginia 22217		10. PROGRAM ELEMENT, PROJECT, TASK AREA & WORK UNIT NUMBERS NRL Problem H02-28A	
11. MONITORING AGENCY NAME & ADDRESS (if different from Controlling Office) 12-17p.		12. REPORT DATE April 1978	
		13. NUMBER OF PAGES 16	
		14. SECURITY CLASS. (of this report) UNCLASSIFIED	
15. DISTRIBUTION STATEMENT (of this Report) Approved for public release; distribution unlimited.		15a. DECLASSIFICATION DOWNGRADING SCHEDULE	
16. DISTRIBUTION STATEMENT (of the abstract entered in Block 20, if different from Report)			
17. SUPPLEMENTARY NOTES *NRC Research Associate at Naval Research Laboratory			
18. KEY WORDS (Continue on reverse side if necessary and identify by block number) Argon-nitrogen laser Energy transfer laser Intense proton beams Proton beam pumped laser			
19. ABSTRACT (Continue on reverse side if necessary and identify by block number) Gas laser action using a charge and current neutralized proton beam as a pump source has been demonstrated. Stimulated emission at 357.7 and 380.5 nm, corresponding to the $v' = 0 \rightarrow v'' = 1$ and $v' = 0 \rightarrow v'' = 2$ transitions of the N ₂ (C → B) band, has been observed in Ar/5%N ₂ gas mixtures. In comparison with electron beams, protons appear to be more efficient for excitation sources of high pressure UV and visible lasers.			

DD FORM 1473

EDITION OF 1 NOV 68 IS OBSOLETE
S. N. 0102-014-6601

SECURITY CLASSIFICATION OF THIS PAGE (When Data Entered)

254950

leave as a double prime

CONTENTS

I. INTRODUCTION	1
II. EXPERIMENT	2
III. RESULTS	5
IV. SUMMARY	8
V. ACKNOWLEDGMENTS	8
REFERENCES	9

ACCESSION for	
NTIS	Write Section <input checked="" type="checkbox"/>
DOC	Write Section <input type="checkbox"/>
UNANNOUNCED	<input type="checkbox"/>
JUSTIFICATION.....	
BY.....	
DISTRIBUTION/AVAILABILITY CODES	
Dist.	AVAIL. and/or SPECIAL
A	

PREVIOUS PAGE NOT FILLED
 BLANK

INTENSE PROTON BEAM PUMPED Ar - N₂ LASER

I. INTRODUCTION

Relativistic electron beams have been successfully applied to the excitation of high pressure gas lasers including XeF¹, HgCl², He⁺-N₂ → N₂⁺ (B → X)³ and Ar-N₂ at 357.7 nm.⁴⁻⁸ All of these lasers rely on the production of rare gas ions to ultimately produce the population in the upper laser level. However, since the ionization cross-section of the rare gases by proton impact is larger than for electrons of the same energy,⁹ it has been recently suggested¹⁰ that proton beams may surpass electrons in efficiently pumping lasers of current interest.

During the past four years, a variety of sources has been developed for the production of intense proton beams. Parameters typical of these beams¹¹⁻¹⁷ are proton energies of 0.1 - 1.5 MeV, currents of 1 - 300 kA, and current densities of 0.01 - 70 kA/cm.² Devices for generating these beams include reflex triodes,^{11,13} pinched electron diodes,¹⁴ magnetically insulated diodes,^{15,16} and most recently, the reflex tetrode.^{17,18} The reflex tetrode is of particular interest since ion beam generation efficiencies ≥ 50% can be achieved with high current density (≥ 1kA/cm²) utilizing a moderate impedance (e.g. 7 Ohms) pulse generator. The efficient generation of proton beams by reflex tetrodes makes attractive the use of protons for the excitation of gas lasers.

Note: Manuscript submitted March 22, 1978.

Several proposals, incorporating the attractive features of ion beams, including a swept-gain ion pumped laser¹⁹ and a charge exchange oscillator for XUV wave lengths,²⁰ have appeared in the literature.

The first demonstration of gas laser action by excitation with a charge and current neutralized proton beam is reported in this paper. Stimulated emission at 357.7 and 380.5 nm, corresponding to the $v' = 0 \rightarrow v'' = 1$ and $v' = 0 \rightarrow v'' = 2$ transitions of the N_2 (C \rightarrow B) band, respectively, has been observed in Ar/ N_2 gas mixtures. Measurements of the laser and proton beam deposition energies indicate that ion excitation is indeed a more efficient pump than its e-beam counterpart. Evidence of lasing action in the Ar/ N_2 gas mixture consists of temporal, spatial and frequency narrowing of the N_2 (C \rightarrow B) spontaneous emission. The dependence of laser output on gas pressure and the delay of lasing with respect to the pump pulse are similar to those obtained previously using electron beam excitation.

II. EXPERIMENT

A partial schematic diagram of the experimental apparatus is shown in Fig. 1. The proton beam, which is generated by a reflex tetrode^{17,18} powered by the Seven Ohm Line (SOL) Generator at the Naval Research Laboratory, is injected into a high pressure gas cell through a 3- μ m thick mylar window. The laser axis is defined by an optical cavity oriented perpendicular to the proton beam.

The reflex tetrode consists of a grounded carbon cathode K of

5.0 cm diam. and two anodes to which a positive voltage pulse of 450 kV and 50 ns duration (FWHM) is applied. The first anode A_1 consists of a 6.3- μm thick aluminized mylar foil spaced 2.2 cm from the cathode. The second anode A_2 is a 12.5- μm -thick polyethylene film spaced 6 mm from A_1 . An axial magnetic field of 5.6 kG is applied along the axis of the tetrode, and the pressure in the vacuum chamber is maintained at less than 0.9 milliTorr.

When the pulse is applied to the anodes, electrons are emitted from the cathode, accelerate to and penetrate the anodes and form a virtual cathode downstream. As the electrons reflex between virtual and real cathodes, plasma is formed on A_2 , and protons are accelerated toward the virtual cathode. As the protons exit the virtual cathode and form a drifting beam, electrons are dragged along. Thus the proton beam is: 1) space charge and current neutralized and 2) unidirectional, i.e., traveling away from the diode.

The proton beam propagates 24 cm to the mylar window of the gas cell. After passing through the window, the incident 450 keV protons emerge with approximately 200 keV energy.²¹ With ~ 1 atmosphere of gas in the cell, the proton range is 5 mm. The laser cell was machined from polyvinyl chloride (PVC) and includes demountable Brewster angle Suprasil (VUV quality) quartz windows. All O-rings are made of Viton or silicone rubber. The vacuum system used to evacuate the laser cell is constructed of stainless-steel and all gas lines are Teflon tubing to maintain gas purity. After pumping the laser cell to $< 10^{-2}$ Torr, it is filled with a Ar/5% N_2 gas mixture, with total pressures P_{TOTAL} ranging from 1 to 1.5 atm.

The 3- μm thick proton beam window is sandwiched between two

rectangular aluminum rings with silicone rubber sealant. Since a new foil is required for each shot, this mylar-aluminum assembly facilitates rapid foil replacement. The foil assembly is vacuum sealed to a silicone O-ring with pressure supplied by another O-ring behind the assembly. The foil rests against a support plate (not shown in Fig. 1) machined from aluminum with a honeycomb array of 4 mm diameter holes permitting ~50% transmission of the p-beam.

The optical cavity consists of two highly reflecting dielectric mirrors ($R \sim 99.8\%$, $T \sim 0.1\%$ at 357 nm) of 5 m radius of curvature separated by 70 cm. Laser and spontaneous emission spectra are obtained by an S-5 surface photodiode and neutral density filters placed ~ 1 m from the laser cavity. To insure the accuracy of laser energy measurements, the photodiode was calibrated against a carbon calorimeter and an XeF discharge laser emitting 1.5 mJ at 351 and 353 nm. At the other end of the laser resonator, a 1 m Czerny-Turner spectrograph (in first order, 8.3 \AA/mm) views the Ar-N₂ laser and spontaneous emission spectra with resolution of 0.2 \AA and 1.6 \AA , respectively. The spectra are recorded on Polaroid Type 55 film and the negatives are scanned using a Joyce-Loebl microdensitometer.

The number of protons impinging on the mylar window of the cell is determined by nuclear activation techniques.²² A thick boron nitride target is positioned behind the support plate in the laser cell. When protons with energies above 277 keV strike the target, a small fraction of the protons induce the resonant nuclear reaction $^{14}\text{N}(p,\gamma)^{15}\text{O}$ in the target. The number of ^{15}O nuclei is measured by coincidence counting the γ rays that are produced from the annihilation of positrons emitted

in the decay of ^{15}O . Typically, 1.5×10^{12} protons/cm² per pulse are incident on the mylar window, giving a total beam energy into the gas cell of ~ 0.5 J (support plate "open" area ≈ 11 cm²).

III. RESULTS

Densitometer tracings of the spontaneous and laser emission spectra are given in Fig. 2 where 2(a) shows the fluorescence spectrum obtained with one cavity mirror in place. Since the transition probabilities for the N_2 (C \rightarrow B) (0,0), (0,1) and (0,2) lines are in the ratio 12:8.6:0.3,²³ amplified spontaneous emission is clearly being observed. With the addition of the second mirror, the intensity at 357.7 and 380.5 nm rises by over two orders of magnitude and considerable spectral narrowing takes place as shown in Fig. 2(b).

An estimate of the divergence of the laser beam is made using open-shutter photography. Exposed Polaroid film which fluoresces blue light when irradiated by ultraviolet radiation is placed 1 m from one mirror. The spot size is found to be 1.3 cm in diameter giving a beam divergence of ≤ 13 milliradians.

Figure 3 illustrates the temporal behavior of the fluorescence and laser emission. With a 1 atm., Ar/5% N_2 gas mixture in the laser cell, maximum fluorescence (no mirrors) occurs ~ 70 ns after initiation of the reflex tetrode voltage pulse (cf. Fig. 3b). Adding the optical cavity produces the laser pulse of Fig. 3c which is delayed by ~ 40 ns from peak spontaneous emission. For 1.5 atm mixture pressure, an ~ 40 ns FWHM laser waveform is observed which is characteristic of a gain-switched pulse (Fig. 3d). The leading edge of the spike occurs early in the

fluorescence. The laser pulse energy more than doubles when P_{TOTAL} is increased from 1.0 to 1.5 atm. This behavior is typical of that previously reported for electron-beam pumped Ar-N₂ lasers.⁴

As shown in Fig. 3a, the potential pulse applied to the anode of the reflex tetrode reverses polarity after 60 ns and a beam of energetic electrons is generated. Electrons, with energy ~ 135 keV, a peak current density ≤ 50 A/cm² and risetime for the current of ~ 40 ns, reach the gas cell. Therefore, it is necessary to distinguish between excitation of the laser by the proton beam and by the later pulse of energetic electrons.

Comparison was made between laser emission observed when both the neutralized proton beam and the later electron pulse irradiated the gas mixture (Fig. 3c) and when only the energetic electrons were allowed to enter the gas cell (Fig. 3e). Without blocking of the p-beam, laser emission (Fig. 3c) begins ~ 85 ns after the start of the voltage pulse. After subtracting the delay for production of protons at the tetrode (~ 15 ns) and the ion beam time of flight (~ 22 ns), the time lapse between the arrival of the protons and laser emission is found to be ~ 48 ns ($P_{\text{TOTAL}} = 1$ atm). The proton beam was blocked by placing a 12.5 μm thick aluminized mylar film which is equivalent to twice the range of a 450 keV proton, on the tetrode side of the gas laser cell's mylar window. Figure 3e shows the laser pulse obtained when the protons were stopped prior to entering the cell. Stimulated emission appears ~ 100 ns after the energetic electron pulse begins and approximately 60 ns after peak electron flux. Therefore, the laser waveforms of Figs. 3c and d are due to proton beam pumping. Further evidence that

the laser described here is pumped by the protons lies in the observations that the C \rightarrow B fluorescence starts 10 ns prior to the termination of the positive portion of the anode voltage. Also, for 1.5 atm. in the gas cell, the laser pulse of Fig. 3d begins \sim 15 ns after the arrival of the protons and \leq 10 ns after polarity reversal of the voltage, at which time the electron flux is small.

Following excitation by the proton beam, re-excitation by the later electron pulse is not observed. This is perhaps a consequence of the \sim 10 μ sec lifetime of the lower level of the laser transition which inhibits further inversion.

Maximum laser energy is obtained at $P_{\text{TOTAL}} = 1.5$ atm., the highest studied in these experiments due to the thin mylar window. (Smaller diameter holes in the foil support plate or higher applied voltages and thicker windows will permit investigation of higher mixture pressures.) At this pressure with a cavity output coupling of 0.1%, \geq 0.02 mJ of laser energy is extracted.

Higher output coupling obtained by using a mirror with 10 - 20% transmission (as commonly used in e-beam pumping experiments⁵) may yield laser energies of 2-5 mJ per pulse. Since \approx 0.5 J of proton energy enters the gas cell, careful design of the optical resonator might yield efficiencies approaching 1%, $2\frac{1}{2}$ times higher than those previously reported for the transverse, e-beam pumped Ar-N₂ laser.^{5,6} Also, the $\frac{1}{2}$ J of protons impinging on the gas are delivered over a 9 cm \times 2.3 cm cross-sectional area whereas the optical cavity used in the present experiments defines the diameter of the lasing volume as $\sim \frac{1}{2}$ mm. Therefore, the majority of the excited cell volume is not used.

IV. SUMMARY

In summary, the demonstration of the first proton beam-pumped laser has been achieved. Further work on Ar-N₂, using higher output coupling mirrors to increase the extracted energy, is in progress. The large rates of ionization of argon (as well as the other rare gases) by high energy protons (200-500 keV) and the resulting energy depositions available (i.e. dE/dx) suggests that the design of powerful and efficient ($\eta \sim 1 - 10\%$) molecular lasers such as the rare gas-halides is feasible. Finally, since the modification of existing e-beam machines to proton beam accelerators (with a reflex tetrode) is straightforward, proton beam pumping of gas lasers appears to be an attractive alternative to e-beam excitation.

V. ACKNOWLEDGMENTS

The authors are grateful to D. Epp for designing portions of the laser cell and foil assembly and to R. Covington for technical assistance.

This work is supported by ONR and DOE.

References

1. C. A. Brau and J. J. Ewing, Appl. Phys. Lett. 27, 435 (1975); L. F. Champagne, J. G. Eden, N. W. Harris, N. Djeu, and S. K. Searles, Appl. Phys. Lett. 30, 160 (1977); L. F. Champagne and N. W. Harris, Appl. Phys. Lett. 31, 513 (1977).
2. J. H. Parks, Appl. Phys. Lett. 31, 192 (1977); J. G. Eden, Appl. Phys. Lett. 31, 448 (1977).
3. C. B. Collins, A. J. Cunningham, S. M. Curry, B. W. Johnson, and M. Stockton, Appl. Phys. Lett. 24, 477 (1974).
4. S. K. Searles and G. A. Hart, Appl. Phys. Lett. 25, 79 (1974).
5. E. R. Ault, M. L. Bhaumik, and N. T. Olson, IEEE J. of Quant. Elect., QE-10, 624 (1974).
6. N. G. Basov, V. A. Danilychev, V. A. Dolgikh, O. M. Kerimov, A. N. Dobanov, and A. F. Suchkov, JETP Lett. 20, 53 (1974).
7. S. K. Searles, Appl. Phys. Lett. 25, 735 (1974).
8. N. G. Basov, A. N. Brunin, V. A. Danilychev, V. A. Dolgikh, O. M. Kerimov, A. N. Lobanov, S. I. Sagitov, and A. F. Suchkov, Sov. J. Quant. Elect., 2, 1218 (1976). Original published 1975.
9. E. W. McDaniel, Collision Phenomena in Ionized Gases, John Wiley and Sons, Inc., New York (1964).
10. A. W. Ali, Memo Report 3519, Naval Research Laboratory, Wash., D. C., (1977); J. Appl. Phys. 49, 920 (1978).
11. J. Golden, C. A. Kapetanacos, S. J. Marsh, and S. J. Stephanakis, Phys. Rev. Lett. 38, 130 (1977); also C. A. Kapetanacos, J. Golden, and W. M. Black, Phys. Rev. Lett. 37, 1236 (1976).

12. S. Humphries, J. J. Lee, and R. N. Sudan, Appl. Phys. Lett. 25, 20 (1974).
13. D. S. Prono, J. W. Shearer, and R. J. Briggs, Phys. Rev. Lett. 37, 21 (1976).
14. S. J. Stephanakis, D. Mosher, G. Cooperstein, J. R. Boller, J. Golden, and S. A. Goldstein, Phys. Rev. Lett. 37, 1543 (1976);
D. Mosher, G. Cooperstein, S. J. Stephanakis, S. A. Goldstein, D. G. Colombant, R. Lee, 2nd Int. Top. Conf. on High Power Electron and Ion Beam Res. and Tech., Cornell Univ., Ithaca, N. Y. (1977).
15. M. Greenspan, S. Humphries, J. Maenchen, and R. N. Sudan, Phys. Rev. Lett. 39, 24 (1977).
16. S. C. Luckhardt and H. H. Fleischmann, Appl. Phys. Lett. 30, 182 (1977).
17. J. A. Pasour, R. A. Mahaffey, J. Golden, and C. A. Kapetanacos, Phys. Rev. Lett. 40, 448 (1978).
18. R. A. Mahaffey, J. A. Pasour, J. Golden, and C. A. Kapetanacos, Appl. Phys. Lett. 32 (1978).
19. W. H. Louisell, M. O. Scully, and W. B. McKnight, Phys. Rev. A11, 989 (1975).
20. A. W. Ali, J. Golden, C. A. Kapetanacos, and R. W. Waynant, Memo Report 3064, NRL, Wash. D. C. (1975).
21. L. C. Northcliffe and R. F. Schilling, Nuc. Data Tables A7, 233 (1970).
22. F. C. Young, J. Golden, and C. A. Kapetanacos, Rev. Sci. Instrum. 48, 432 (1977).
23. A. W. Johnson and R. G. Fowler, J. Chem. Phys. 53, 65 (1970).

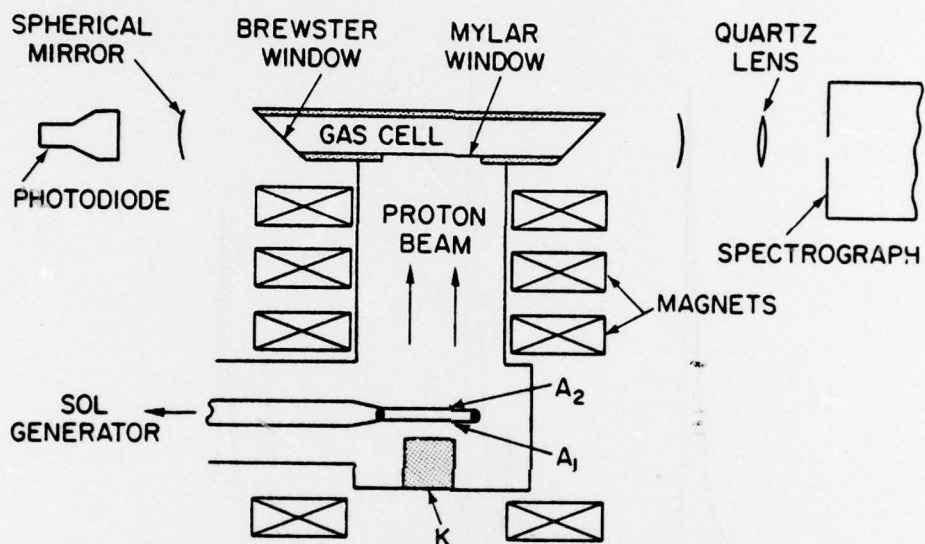


Fig. 1 — Schematic diagram of the proton beam device, laser cell and optics. The carbon cathode is represented by K, the aluminized mylar anode by A₁, and the polyethylene foil by A₂.

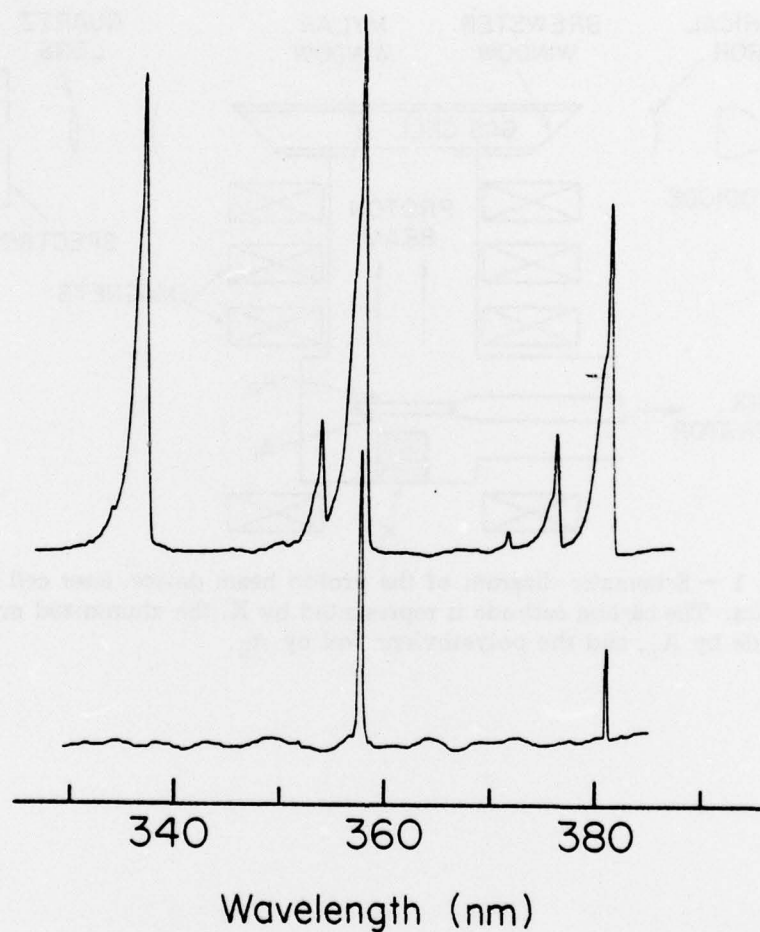


Fig. 2 — Densitometer tracings of the spontaneous (top) and laser emission spectra for spectrograph resolution of 1.6\AA and 0.2\AA , respectively. The 337.1, 357.7 and 380.5 nm bands correspond to the (0,0), (0,1) and (0,2) lines of the N_2 ($C \rightarrow B$) transition.

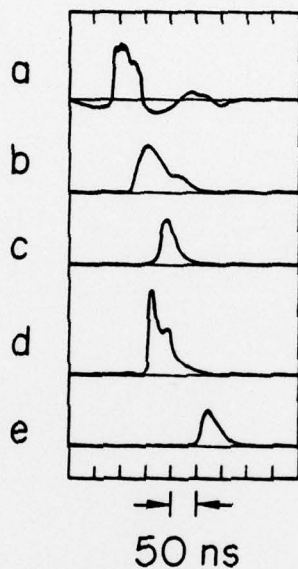


Fig. 3 — Waveforms pertinent to the proton beam excited Ar-N₂ laser: a. Anode voltage (not inductively corrected)-peak voltage ≈ 520 kV; b. Fluorescence from a 1 atm total pressure mixture of 95% Ar/5% N₂ composition; c. Laser pulse, $P_{\text{TOTAL}} = 1.0$ atm; d. Laser pulse, $P_{\text{TOTAL}} = 1.5$ atm; e. Stimulated emission obtained with the proton beam blocked by 12.5 μm thickness aluminized mylar foil. [Horizontal scale: 50ns/div; vertical units arbitrary.]